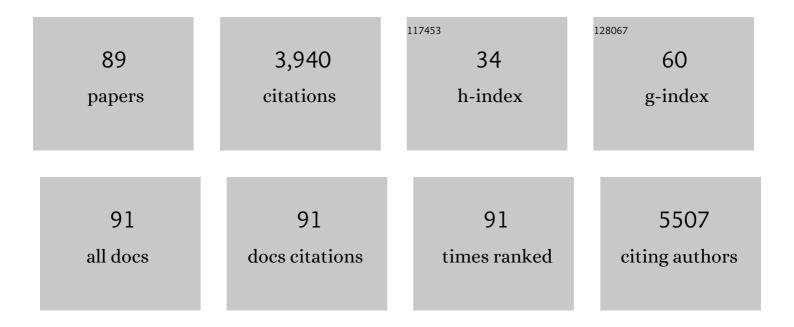
List of Publications by Year in descending order

Source: https://exaly.com/author-pdf/2323954/publications.pdf Version: 2024-02-01



Ηλιμιάνι Ι

#	Article	IF	CITATIONS
1	High-Entropy Oxide for Highly Efficient Luminol–Dissolved Oxygen Electrochemiluminescence and Biosensing Applications. Analytical Chemistry, 2022, 94, 2958-2965.	3.2	22
2	Photoactivated Bacteriorhodopsin/SiN _{<i>x</i>} Nanopore-Based Biological Nanofluidic Generator with Single-Protein Sensitivity. ACS Nano, 2022, 16, 1589-1599.	7.3	7
3	Plasmon-Enhanced Nitrogen Vacancy-Rich Carbon Nitride Electrochemiluminescence Aptasensor for Highly Sensitive Detection of miRNA. Analytical Chemistry, 2022, 94, 1406-1414.	3.2	23
4	Smart Tumor Microenvironment-Responsive Nano-Prodrug for Disulfiram Toxification In Situ and the Exploration of Lethal Mechanisms in Cells. Langmuir, 2022, 38, 584-592.	1.6	6
5	Magic-sized CdSe nanoclusters for efficient visible-light-driven hydrogen evolution. Nano Research, 2022, 15, 3106-3113.	5.8	16
6	Optoplasmonic Modulation of Cell Metabolic State Promotes Rapid Cell Differentiation. Analytical Chemistry, 2022, 94, 8354-8364.	3.2	4
7	Gold nanoparticle-based signal amplified electrochemiluminescence for biosensing applications. Talanta, 2022, 248, 123611.	2.9	18
8	Thermoplasmonic Regulation of the Mitochondrial Metabolic State for Promoting Directed Differentiation of Dental Pulp Stem Cells. Analytical Chemistry, 2022, 94, 9564-9571.	3.2	9
9	Plasmon-enhanced quantum dots electrochemiluminescence aptasensor for selective and sensitive detection of cardiac troponin I. Talanta, 2021, 221, 121674.	2.9	34
10	Shellâ€Isolated Plasmonic Nanostructures for Biosensing, Catalysis, and Advanced Nanoelectronics. Advanced Functional Materials, 2021, 31, 2008031.	7.8	17
11	Electrochemiluminescence of Ru(bpy) ₃ ²⁺ /thioacetamide and its application for the sensitive determination of hepatotoxic thioacetamide. Analyst, The, 2021, 146, 5198-5203.	1.7	5
12	Glutathione Content Detection of Single Cells under Ingested Doxorubicin by Functionalized Glass Nanopores. Analytical Chemistry, 2021, 93, 4240-4245.	3.2	40
13	Two-Dimensional-Plasmon-Boosted Iron Single-Atom Electrochemiluminescence for the Ultrasensitive Detection of Dopamine, Hemin, and Mercury. Analytical Chemistry, 2021, 93, 9949-9957.	3.2	42
14	Light Scattering and Luminophore Enrichment-Enhanced Electrochemiluminescence by a 2D Porous Ru@SiO ₂ Nanoparticle Membrane and Its Application in Ultrasensitive Detection of Prostate-Specific Antigen. Analytical Chemistry, 2021, 93, 11641-11647.	3.2	25
15	Wet-Chemical Electro-Plasmonic Modulation of Metasurfaced Cell–Electrode Interfaces for Effective and Selective Entropic Killing of Cancer Cells. Analytical Chemistry, 2021, 93, 13624-13631.	3.2	2
16	Label-Free Single-Particle Surface-Enhanced Raman Spectroscopy Detection of Phosphatidylserine Externalization on Cell Membranes with Multifunctional Micron-Nano Composite Probes. Analytical Chemistry, 2021, 93, 2183-2190.	3.2	21
17	Label-Free Analysis of Cell Membrane Proteins via Evanescent Field Excited Surface-Enhanced Raman Scattering. Journal of Physical Chemistry Letters, 2021, 12, 10720-10727.	2.1	2
18	Plasmon-Boosted Cu-Doped TiO ₂ Oxygen Vacancy-Rich Luminol Electrochemiluminescence for Highly Sensitive Detection of Alkaline Phosphatase. Analytical Chemistry, 2021, 93, 15183-15191.	3.2	25

#	Article	IF	CITATIONS
19	High-efficiency cathodic electrochemiluminescence of the tris(2,2′-bipyridine)ruthenium(<scp>ii</scp>)/ <i>N</i> -hydroxy compound system and its use for sensitive "turn-on―detection of mercury(<scp>ii</scp>) and methyl blue. Chemical Communications, 2020, 56, 1827-1830.	2.2	12
20	Single-cell ATP detection and content analyses in electrostimulus-induced apoptosis using functionalized glass nanopipettes. Chemical Communications, 2020, 56, 1561-1564.	2.2	38
21	A green, efficient and precise hydrogen therapy of cancer based on <i>in vivo</i> electrochemistry. National Science Review, 2020, 7, 660-670.	4.6	25
22	Quasi-Photonic Crystal Light-Scattering Signal Amplification of SiO ₂ -Nanomembrane for Ultrasensitive Electrochemiluminescence Detection of Cardiac Troponin I. Analytical Chemistry, 2020, 92, 845-852.	3.2	26
23	Programmable Organicâ€Free Negative Differential Resistance Memristor Based on Plasmonic Tunnel Junction. Small, 2020, 16, e2002727.	5.2	11
24	Plasmonic SERS Au Nanosunflowers for Sensitive and Label-Free Diagnosis of DNA Base Damage in Stimulus-Induced Cell Apoptosis. Analytical Chemistry, 2020, 92, 11755-11762.	3.2	37
25	Fast Activation and Tracing of Caspase-3 Involved Cell Apoptosis by Combined Electrostimulation and Smart Signal-Amplified SERS Nanoprobes. Analytical Chemistry, 2020, 92, 7861-7868.	3.2	28
26	Glucose level determination in single cells in their satiety and starvation states using an enzymatic functional glass nanopore. Chemical Communications, 2020, 56, 5393-5396.	2.2	21
27	Tumor Microenvironment-Activated Degradable Multifunctional Nanoreactor for Synergistic Cancer Therapy and Glucose SERS Feedback. IScience, 2020, 23, 101274.	1.9	30
28	Molecular Profiling of Dental Pulp Stem Cells during Cell Differentiation by Surface Enhanced Raman Spectroscopy. Analytical Chemistry, 2020, 92, 3735-3741.	3.2	14
29	Single-Cell Adenosine Triphosphate Content Monitoring during Hyperthermia Cell Death by Using Plasmonic Fluorescent Nanoflare. Analytical Chemistry, 2020, 92, 3882-3887.	3.2	10
30	Oriented bacteriorhodopsin/polyaniline hybrid bio-nanofilms as photo-assisted electrodes for high performance supercapacitors. Journal of Materials Chemistry A, 2020, 8, 8268-8272.	5.2	16
31	Self-supporting MOF-derived CoNi@C–Au/TiO ₂ nanotube array Z-scheme heterocatalysts for plasmon-enhanced high-efficiency full water splitting. Journal of Materials Chemistry A, 2019, 7, 19704-19708.	5.2	23
32	Nanoengineered Metasurface Immunosensor with over 1000-Fold Electrochemiluminescence Enhancement for Ultra-sensitive Bioassay. IScience, 2019, 17, 267-276.	1.9	31
33	Living-Cell Imaging of Mitochondrial Membrane Potential Oscillation and Phenylalanine Metabolism Modulation during Periodic Electrostimulus. Analytical Chemistry, 2019, 91, 9571-9579.	3.2	29
34	Enzymatic Preparation of Plasmonic-Fluorescent Quantum Dot-Gold Hybrid Nanoprobes for Sensitive Detection of Glucose and Alkaline Phosphatase and Dual-Modality Cell Imaging. Analytical Chemistry, 2019, 91, 14074-14079.	3.2	14
35	Modulating Catalytic Performance of Metal–Organic Framework Composites by Localized Surface Plasmon Resonance. ACS Catalysis, 2019, 9, 11502-11514.	5.5	61
36	Efficient Electrogenerated Chemiluminescence of Tris(2,2′-bipyridine)ruthenium(II) with <i>N</i> -Hydroxysulfosuccinimide as a Coreactant for Selective and Sensitive Detection of <scp>l</scp> -Proline and Mercury(II). Analytical Chemistry, 2019, 91, 12517-12524.	3.2	47

#	Article	IF	CITATIONS
37	Smart Plasmonic Nanozyme Enhances Combined Chemo-photothermal Cancer Therapy and Reveals Tryptophan Metabolic Apoptotic Pathway. Analytical Chemistry, 2019, 91, 12203-12211.	3.2	28
38	Lucigenin-Tris(2-carboxyethyl)phosphine Chemiluminescence for Selective and Sensitive Detection of TCEP, Superoxide Dismutase, Mercury(II), and Dopamine. Analytical Chemistry, 2019, 91, 3070-3077.	3.2	27
39	Enhancing Luminol Electrochemiluminescence by Combined Use of Cobalt-Based Metal Organic Frameworks and Silver Nanoparticles and Its Application in Ultrasensitive Detection of Cardiac Troponin I. Analytical Chemistry, 2019, 91, 3048-3054.	3.2	113
40	Recent advances in nanomaterialâ€based capillary electrophoresis. Electrophoresis, 2019, 40, 2050-2057.	1.3	20
41	Resistive-Pulse Sensing and Surface Charge Analysis of a Single Nanoparticle Collision at a Conical Class Nanopore. Analytical Chemistry, 2019, 91, 7648-7653.	3.2	13
42	Short-chain oligonucleotide detection by glass nanopore using targeting-induced DNA tetrahedron deformation as signal amplifier. Analytica Chimica Acta, 2019, 1063, 57-63.	2.6	12
43	Unprecedented efficient electron transport across Au nanoparticles with up to 25-nm insulating SiO2-shells. Scientific Reports, 2019, 9, 18336.	1.6	9
44	Enhancing Photothermal Effect and Stability of Plasmonic Pd/Agâ€Nanosheet by Nanoassembly for Efficient Lightâ€Đriven Catalytic Organic Hydrogenation. ChemistrySelect, 2019, 4, 13173-13181.	0.7	4
45	Single-Molecule Translocation Conformational Sensing of Multiarm DNA Concatemers Using Glass Capillary Nanopore. ACS Sensors, 2019, 4, 3119-3123.	4.0	11
46	A Ternary Pt/Au/TiO ₂ â€Decorated Plasmonic Wood Carbon for Highâ€Efficiency Interfacial Solar Steam Generation and Photodegradation of Tetracycline. ChemSusChem, 2019, 12, 467-472.	3.6	88
47	Smart Plasmonic Nanorobot for Real-Time Monitoring Cytochrome c Release and Cell Acidification in Apoptosis during Electrostimulation. Analytical Chemistry, 2019, 91, 1408-1415.	3.2	48
48	Bifunctional plasmonic colloidosome/graphene oxide-based floating membranes for recyclable high-efficiency solar-driven clean water generation. Nano Research, 2018, 11, 3854-3863.	5.8	35
49	PVP-coated gold nanoparticles for the selective determination of ochratoxin A via quenching fluorescence of the free aptamer. Food Chemistry, 2018, 249, 45-50.	4.2	41
50	Pd/Ag nanosheet as a plasmonic sensing platform for sensitive assessment of hydrogen evolution reaction in colloid solutions. Nano Research, 2018, 11, 2093-2103.	5.8	13
51	Adaption of a Solid-State Nanopore to Homogeneous DNA Organization Verification and Label-Free Molecular Analysis without Covalent Modification. Analytical Chemistry, 2018, 90, 814-820.	3.2	36
52	Plasmonics Yields Efficient Electron Transport via Assembly of Shell-Insulated Au Nanoparticles. IScience, 2018, 8, 213-221.	1.9	27
53	Controlled Decoration of Divalent Nickel onto CdS/CdSe Core/Shell Quantum Dots to Boost Visibleâ€Lightâ€Induced Hydrogen Generation in Water. ChemPlusChem, 2018, 83, 1088-1096.	1.3	3
54	Boosting Electrocatalytic Oxygen Evolution Performance of Ultrathin Co/Ni-MOF Nanosheets via Plasmon-Induced Hot Carriers, ACS Applied Materials & app: Interfaces, 2018, 10, 37095-37102	4.0	67

#	Article	IF	CITATIONS
55	Nucleus and Mitochondria Targeting Theranostic Plasmonic Surface-Enhanced Raman Spectroscopy Nanoprobes as a Means for Revealing Molecular Stress Response Differences in Hyperthermia Cell Death between Cancerous and Normal Cells. Analytical Chemistry, 2018, 90, 13356-13364.	3.2	50
56	Plasmon-driven water splitting enhancement on plasmonic metal–insulator–semiconductor hetero-nanostructures: unraveling the crucial role of interfacial engineering. Nanoscale, 2018, 10, 14290-14297.	2.8	25
57	Single-cell pH imaging and detection for pH profiling and label-free rapid identification of cancer-cells. Scientific Reports, 2017, 7, 1759.	1.6	56
58	Controllable Shrinking of Glass Capillary Nanopores Down to sub-10 nm by Wet-Chemical Silanization for Signal-Enhanced DNA Translocation. ACS Sensors, 2017, 2, 1452-1457.	4.0	31
59	Shell Thickness Engineering Significantly Boosts the Photocatalytic H ₂ Evolution Efficiency of CdS/CdSe Core/Shell Quantum Dots. ACS Applied Materials & Interfaces, 2017, 9, 35712-35720.	4.0	48
60	Long-Range Plasmon Field and Plasmoelectric Effect on Catalysis Revealed by Shell-Thickness-Tunable Pinhole-Free Au@SiO ₂ Core–Shell Nanoparticles: A Case Study of <i>p</i> -Nitrophenol Reduction. ACS Catalysis, 2017, 7, 5391-5398.	5.5	73
61	Free-Standing Monolayered Metallic Nanoparticle Networks as Building Blocks for Plasmonic Nanoelectronic Junctions. ACS Applied Materials & Interfaces, 2016, 8, 1594-1599.	4.0	14
62	Controllable Fabrication of Transparent Macroporous Graphene Thin Films and Versatile Applications as a Conducting Platform. Advanced Functional Materials, 2015, 25, 4334-4343.	7.8	25
63	Facile One-Step Photochemical Fabrication and Characterization of an Ultrathin Gold-Decorated Single Glass Nanopipette. Analytical Chemistry, 2015, 87, 3216-3221.	3.2	48
64	Smart Plasmonic Glucose Nanosensors as Generic Theranostic Agents for Targeting-Free Cancer Cell Screening and Killing. Analytical Chemistry, 2015, 87, 6868-6874.	3.2	37
65	Single glass nanopore-based regenerable sensing platforms with a non-immobilized polyglutamic acid probe for selective detection of cupric ions. Analytica Chimica Acta, 2015, 889, 98-105.	2.6	28
66	Self-standing non-noble metal (Ni–Fe) oxide nanotube array anode catalysts with synergistic reactivity for high-performance water oxidation. Journal of Materials Chemistry A, 2015, 3, 7179-7186.	5.2	96
67	Graphene Oxide-Supported Ag Nanoplates as LSPR Tunable and Reproducible Substrates for SERS Applications with Optimized Sensitivity. ACS Applied Materials & Interfaces, 2015, 7, 18038-18045.	4.0	65
68	Multifunctional Compact Hybrid Au Nanoshells: A New Generation of Nanoplasmonic Probes for Biosensing, Imaging, and Controlled Release. Accounts of Chemical Research, 2014, 47, 138-148.	7.6	107
69	A Highâ€Performance Binary Ni–Co Hydroxideâ€based Water Oxidation Electrode with Threeâ€Dimensional Coaxial Nanotube Array Structure. Advanced Functional Materials, 2014, 24, 4698-4705.	7.8	348
70	Fluorescent Au nanoclusters: recent progress and sensing applications. Journal of Materials Chemistry C, 2014, 2, 8000-8011.	2.7	133
71	11-Mercaptoundecanoic acid directed one-pot synthesis of water-soluble fluorescent gold nanoclusters and their use as probes for sensitive and selective detection of Cr ³⁺ and Cr ⁶⁺ . Journal of Materials Chemistry C, 2013, 1, 138-143.	2.7	116
72	Facile and rapid synthesis of water-soluble fluorescent gold nanoclusters for sensitive and selective detection of Ag ⁺ . Journal of Materials Chemistry C, 2013, 1, 908-913.	2.7	78

#	Article	IF	CITATIONS
73	Engineering Plasmonic Gold Nanostructures and Metamaterials for Biosensing and Nanomedicine. Advanced Materials, 2012, 24, 5153-5165.	11.1	128
74	Controlled synthesis of porous Ag/Au bimetallic hollow nanoshells with tunable plasmonic and catalytic properties. Nano Research, 2012, 5, 135-144.	5.8	108
75	Effect of hydroxyl and amino groups on electrochemiluminescence activity of tertiary amines at low tris(2,2′-bipyridyl)ruthenium(II) concentrations. Talanta, 2010, 81, 44-47.	2.9	40
76	Electrochemiluminescence of tris(2,2′-bipyridyl)ruthenium(ii)/pyruvate system in the absence of cerium(iii). Analytical Methods, 2010, 2, 479.	1.3	8
77	Determination of isocyanates by capillary electrophoresis with tris(2,2′â€bipyridine)ruthenium(II) electrochemiluminescence. Electrophoresis, 2009, 30, 3926-3931.	1.3	20
78	Electrochemiluminescence from tris(2,2′-bipyridyl)ruthenium(II)–graphene–Nafion modified electrode. Talanta, 2009, 79, 165-170.	2.9	129
79	CEC with tris(2,2′â€bipyridyl) ruthenium(II) electrochemiluminescent detection. Electrophoresis, 2008, 29, 4475-4481.	1.3	13
80	Seed-Mediated Growth of Nearly Monodisperse Palladium Nanocubes with Controllable Sizes. Crystal Growth and Design, 2008, 8, 4440-4444.	1.4	230
81	Environmentally Friendly and Highly Sensitive Ruthenium(II) Tris(2,2′-bipyridyl) Electrochemiluminescent System Using 2-(Dibutylamino)ethanol as Co-Reactant. Angewandte Chemie - International Edition, 2007, 46, 421-424.	7.2	288
82	Determination of Total Calcium in Plasma by Flow Injection Analysis with Tris(2,2′-bipyridyl)ruthenium(II) Electrochemiluminescent Detection. Electroanalysis, 2006, 18, 1584-1589.	1.5	9
83	Size-dependent aggregates of gold nanoparticles induced by a "molecular fork― New Journal of Chemistry, 2005, 29, 1004.	1.4	4
84	Fabrication and Characterization of DNA/QPVP-Os Redox-Active Multilayer Film. Electroanalysis, 2004, 16, 1931-1937.	1.5	6
85	Robust Core-Shell Supramolecular Assemblies Based on Cationic Vesicles and Ring-Shaped{Mo154} Polyoxomolybdate Nanoclusters: Template-Directed Synthesis and Characterizations. Chemistry - A European Journal, 2004, 10, 3225-3231.	1.7	24
86	Direct Electrochemistry and Surface Plasmon Resonance Characterization of Alternate Layer-by-Layer Self-Assembled DNAâ~'Myoglobin Thin Films on Chemically Modified Gold Surfaces. Langmuir, 2003, 19, 4771-4777.	1.6	48
87	Fabrication of Au(111) single-crystal nanoisland-arrayed electrode ensembles by template-directed seeding growthElectronic supplementary information (ESI) available: cyclic voltammograms. See http://www.rsc.org/suppdata/cc/b2/b204231m/. Chemical Communications, 2002, , 1780-1781.	2.2	16
88	Diffusion-Limited, Aggregation-Based, Mesoscopic Assembly of Roughened Core-Shell Bimetallic Nanoparticles into Fractal Networks at the Air-Water Interface. Angewandte Chemie - International Edition, 2002, 41, 1040-1044.	7.2	46
89	Plasmonic Tunnel Diode and Photodetector based on Layerâ€Stacked AuNPâ€Nanomembrane/pâ€Si Heterojunction. Advanced Electronic Materials, 0, , 2101251.	2.6	3